BMC Pregnancy and Childbirth

RESEARCH

Open Access

Insulin resistance-induced mitochondrial dysfunction and pyroptosis in trophoblasts: protective role of metformin

Runyu Du[1], Yu Bai[1], Ling Li[1], Ying Shao[1] and Na Wu[2*]

Abstract

Background Gestational diabetes mellitus (GDM) affects up to 14% of pregnancies globally, with insulin resistance (IR) playing a critical but often underappreciated role in its pathogenesis. Yet the specific impact of insulin at IR levels on mitochondrial function and pyroptosis in first-trimester trophoblasts remains unclear. Metformin use in GDM pregnancies is rising, but its impact on placental mitochondrial function is uncertain. This study aimed to investigate the impact of IR, a key feature of GDM, on mitochondrial dysfunction and pyroptosis in trophoblasts and to evaluate the protective effects of metformin.

Methods Dual staining assays using TUNEL and caspase-1, and enzyme-linked immunosorbent assay were conducted to assess pyroptosis and pyroptosis-related inflammatory markers in placentas from 42 GDM patients and 39 controls. In vitro, HTR-8/SVneo trophoblast cells were treated with IR-level insulin concentrations, and a concentration gradient of metformin to evaluate the mitochondrial damage, pyroptosis, and cell viability.

Results There was a significant increase in pyroptosis in GDM placenta, as well as pyroptosis-related inflammatory markers, IL-1β and IL-18. Placental IL-1β and IL-18 levels were strongly correlated with IR indices, especially in GDM cases. Moreover, IR-level insulin concentrations induced mitochondrial dysfunction and activated the NLRP3 inflammasome, triggering pyroptosis in HTR-8/SVneo trophoblasts. Metformin, particularly at therapeutic doses (10–100 μM), mitigated IR-induced mitochondrial damage by promoting mitochondrial biogenesis and reducing pyroptosis via suppressing the ROS/TXNIP/NLRP3 pathway. Metformin-treated cells exhibited enhanced mitochondrial respiration, restored membrane potential homeostasis, and reduced oxidative stress.

Conclusion IR, independent of hyperglycemia, drives placental inflammation and trophoblastic injury via pyroptosis. Targeting the ROS/TXNIP/NLRP3 pathway with metformin or other therapeutic agents offers potential therapeutic value in managing IR-related complications in GDM.

Keywords Gestational diabetes mellitus, Insulin resistance, Hyperinsulinemia, Metformin, Pyroptosis, Mitochondria

*Correspondence:
Na Wu
20112246@cmu.edu.cn
[1]Department of Endocrinology, Shengjing Hospital of China Medical University, Shenyang 110004, China
[2]Department of Pediatrics, Shengjing Hospital of China Medical University, Shenyang 110004, China

Introduction

Gestational diabetes mellitus (GDM) is characterized by the first onset or recognition of glucose intolerance during pregnancy, and it poses significant perinatal risks and long-term metabolic challenges for both mothers and their offspring [1]. Affecting 9–14% of pregnancies worldwide [2], GDM has become a growing public health concern, underscoring the need to explore its underlying mechanisms.

While hyperglycemia has traditionally been considered the primary driver of adverse GDM outcomes [1], insulin resistance (IR) plays a crucial yet often underappreciated role in its pathogenesis. Physiological IR during pregnancy supports fetal energy supply, but excessive IR can overwhelm maternal insulin production, leading to GDM [3]. Pre-existing IR, commonly seen in individuals with obesity, polycystic ovary syndrome, or a family history of type 2 diabetes (T2DM), further heightens the risk of developing GDM [4, 5]. For GDM patients unable to manage glucose levels through lifestyle modifications, insulin therapy is frequently prescribed. However, insulin therapy in GDM patients with pre-existing IR can exacerbate hyperinsulinemia. Our previous research indicates that GDM patients on insulin therapy, who typically have higher body mass index (BMI) and a stronger family history of T2DM, experience higher rates of preterm birth and cesarean sections compared to those who can manage GDM through lifestyle interventions [6]. Some researchers have therefore classified GDM into three subtypes: insulin-resistant, insulin-deficient, and mixed [7, 8]. Insulin-resistant GDM is associated with a greater risk of gestational hypertensive disorders [7]. These observations suggest that IR or hyperinsulinemia plays a direct pathogenic role in pregnancy complicated by GDM.

The placenta plays a complex role in pregnancies complicated by GDM, particularly in the presence of IR. Despite systemic IR, the placenta maintains or even enhances its capacity for glucose uptake, ensuring adequate nutrient supply to the fetus [9]. However, if the IR is excessive, placenta-mediated chronic inflammation will occur, contributing to the progression of GDM and its complications [10]. Pyroptosis, a form of programmed cell death that is primarily triggered by activation of the NOD-, LRR- and pyrin domain-containing 3 (NLRP3) inflammasome, leads to caspase-1 activation, cell lysis, and inflammation [11]. This process is overactivated in GDM placentas [12]. Mitochondrial dysfunction, evidenced by structural abnormalities and respiratory issues, has also been observed in GDM placentas [13, 14]. Mitochondrial dysfunction disrupts redox balance, increases reactive oxygen species (ROS) production, and further activates NLRP3, thus promoting pyroptosis [15]. However, the specific impact of hyperinsulinemia associated with IR on mitochondrial function and pyroptosis in first-trimester trophoblasts remains unclear. As these processes directly affect placental function and pregnancy outcomes, further research is needed to clarify their relationship.

Metformin, a first-line treatment for T2DM, is increasingly prescribed during pregnancy for its maternal health benefits [3]. Despite its wide clinical use, the impact of metformin on placental mitochondrial function remains inconclusive. A previous study reported that at therapeutic doses, metformin decreases mitochondrial respiration and oxidative stress in trophoblasts [16]. In contrast, others have claimed that, in trophoblasts, supra-therapeutic concentrations of metformin both increase glycolysis and impair oxidative phosphorylation — the primary means by which glucose is converted to energy in the placenta [17, 18]. Furthermore, the effects seem to vary with maternal conditions; metformin may harm trophoblasts in lean women, but improve those in women with obesity and medication-controlled GDM [18], who often exhibit hyperinsulinemia and IR. In short, we have an incomplete understanding of the impact of metformin on trophoblast mitochondrial function.

The first aim of this study was to explore the effects of IR on placental inflammation by investigating the correlation between pyroptosis-related cytokines and clinical markers, particularly those related to IR. We focused on how insulin, at concentrations typically found in patients with IR, affects mitochondrial function and pyroptosis in first-trimester trophoblasts. A second aim was to examine how varying doses of metformin, combined with insulin at insulin-resistant levels, influence mitochondrial function and pyroptosis. Ultimately, it is hoped that this research provides insights that contribute to improving the management of GDM and mitigating inflammation-mediated complications in insulin-resistant pregnancies.

Materials and methods

Participants

Placental tissues were collected from 39 patients with normal glucose tolerance (NGT) and 42 patients with GDM after cesarean section at Shengjing Hospital of China Medical University. We adopted the inclusion and exclusion criteria as outlined in our earlier study [19]. GDM is diagnosed if, during pregnancy, a 75-g OGTT shows: FPG 5.1-7.0 mmol/L, 1hPG ≥ 10.0 mmol/L, or 2hPG 8.5–11.1 mmol/L. The control group matches the GDM group in age and pre-pregnancy BMI. Exclusions include women under 18 years old, with diabetes history, infectious/inflammatory diseases, hypertension, chronic conditions, multiple pregnancies, or using assisted reproductive technology. The maternal information and data on variable adverse neonatal outcomes were also collected as shown in Table 1. Placental tissues were collected within 30 min of delivery, selecting regions free of

Table 1 Clinical characteristics of patients included in the study

Parameters	NGT ($n=39$)	GDM ($n=42$)	*P* Value
Maternal age (years)	32.67 ± 4.515	32.36 ± 5.291	0.779
Pre-pregnancy weight (kg)	65.5 (56, 72)	65.1 ± 8.745	0.998
Pre-pregnancy BMI (kg/m^2)	24.98 (20.44, 27.34)	25.04 ± 3.776	0.755
Pre-delivery weight (kg)	75.5 (70, 81)	75.57 ± 8.571	0.815
Pre-delivery BMI (kg/m^2)	28.88 (27.34, 31.25)	28.45 (25.53, 31.25)	0.496
Weight gain during pregnancy (kg)	9 (8,10)	12.1 ± 2.721	0.000***
Gravidity history	1 (1, 3)	2 (1, 3)	0.1710
Parity history	0 (0, 1)	0 (0, 1)	0.9053
Gestational age (days)	271 (267, 274)	272 (269, 276)	0.2724
OGTT at diagnosis of GDM or at 24 ~ 28 weeks of gestation			
0 min glucose (mmol/L)	4.533 ± 0.221	5.295 ± 0.562	0.000***
60 min glucose (mmol/L)	7.103 ± 1.276	10.69 (8.963, 11.35)	0.000***
120 min glucose (mmol/L)	6.261 ± 0.9617	8.683 ± 1.675	0.000***
AUC (mmol·L^{-1}·min)	750.5 ± 95.66	1026 ± 144.8	0.000***
FPG at delivery (mmol/L)	4.271 ± 0.501	4.786 ± 0.679	0.000***
HbA1c at delivery (%)	5.329 ± 0.319	5.5 (5.3, 5.8)	0.019*
Fasting insulin at delivery (μU/mL)	11.06 ± 4.193	13.65 (11, 18.28)	0.006**
HOMA-IR at delivery	2.097 ± 0.788	3.047 (2.167, 4.014)	0.001**
logHOMA-IR at delivery	0.715 ± 0.348	1.107 ± 0.404	0.001**
QUIKI at delivery	0.150 ± 0.009	0.141 ± 0.008	0.000***
Baby's sex (female) (n[n%])	19 (48.718%)	21 (50%)	1.000
Birth weight (g)	3502 ± 410.5	3334 ± 549.4	0.1255
Systolic blood pressure	119.8 ± 9.541	116.5 (112.0, 127.3)	0.6557
Diastolic blood pressure	74.62 ± 6.722	74 (70, 83)	0.4001

Abbreviations: NGT: normal glucose tolerance; GDM: gestational diabetes mellitus; BMI: body mass index; OGTT: oral glucose tolerance test; AUC: area under curve; FPG: fasting plasma glucose; HbA1c: glycosylated hemoglobin; HOMA-IR: Homeostasis Model Assessment of Insulin Resistance, calculated as [fasting insulin (μU/mL) × fasting glucose (mmol/L)] / 22.5; QUIKI: Quantitative Insulin Sensitivity Check Index, calculated as 1 / [log(fasting insulin (μU/mL)) + log(fasting glucose (mg/dL))]

Notes Values are presented as mean ± standard deviation for normally distributed variables or median (interquartile range) for non-normally distributed variables or n (n%)

Compared with NGT, *$P<0.05$, **$P<0.01$, ***$P<0.001$

visible calcification and fibrosis. Tissues were rinsed with PBS, snap-frozen for ELISA and Western blot, or fixed in 4% paraformaldehyde for immunofluorescence.

Reagents and antibodies

Tables S1-3 in Supplementary file 1 list the sequence of all target shRNAs or siRNAs, main reagents and instruments, and antibodies used in this study.

Cell culture

Human first-trimester extravillous trophoblast-derived HTR-8/SVneo cells were obtained from the Chinese Academy of Sciences. HTR-8/SVneo cells were cultured in DMEM with 10% FBS in a humidified incubator at 37℃ in 5% CO2, and maintained as adherent monolayers. HTR-8/SVneo cells were incubated for 24 and 48 h with either vehicle control or insulin at concentrations commonly used to induce IR (100 nM and 1000 nM) [20, 21]. For combined treatments, cells were incubated with metformin at concentrations of 10–1000 μM for 24 h following a 48-hour treatment with 1000 nM insulin. For gene knockdown, HTR-8 cells were transfected with either shRNA targeting Gasdermin D (shGSDMD), siRNA of thioredoxin interacting protein (siTXNIP), or control shRNA or siRNA (sh-NC or si-NC). Cells were transfected following protocols and harvested 48 h later. Transfection efficiency was validated by qPCR and Western blot.

TUNEL and Immunofluorescence staining

Placental sections were deparaffinized, rehydrated, and treated with 3% hydrogen peroxide, then permeabilized with proteinase K. DNA fragmentation was assessed using the terminal deoxynucleotidyl transferase mediated dUTP Nick-End labeling (TUNEL) Kit. For immunofluorescence staining, placental sections were incubated with antibodies against Caspase-1, followed by secondary antibodies and DAPI. Images were captured using a Eclipse Ti-sr microscope.

HTR-8 cells were stained with primary anti-TXNIP and anti-NLRP3 antibodies at 4 °C overnight, then with Alexa Fluor-conjugated secondary antibodies at room temperature for 1 h (adjusted for species), and imaged by confocal microscopy. Immunofluorescent staining intensity was evaluated with Image J by selecting regions of interest to measure mean fluorescence intensity, subtracting background, and reporting the average intensity from multiple fields per sample.

Glucose uptake assay

Cells (8×10^5/well in a 6-well plate) were starved of glucose, then incubated with 2-deoxy-glucose. Glucose uptake was quantified by measuring the absorbance at OD412 nm against a standard curve.

Cell viability and LDH release assay

Cells were seeded in 96-well plates at 8,000 cells/well and treated as described. After 24 and 48 h, the Cell Counting Kit-8 solution was added, and absorbance at 450 nm was measured. Cell culture supernatants were collected, incubated with the LDH reaction mixture, and absorbance was measured at 450 nm.

ELISA

IL-1β and IL-18 levels in placental tissues and cell culture supernatants were quantified using ELISA kits. Absorbance was measured at 450 nm with a reference wavelength of 570 nm, and cytokine concentrations were calculated against standard curves.

Western blotting

Total protein was extracted using RIPA buffer, separated by SDS–PAGE, and transferred to PVDF membranes. Membranes were blocked with 5% skimmed milk and incubated overnight at 4 °C with primary antibodies against NLRP3, Gasdermin D (GSDMD) N-terminal fragment, and TXNIP. The membranes were then incubated with secondary antibodies for 1 h at room temperature. Western blot protein bands were analyzed with ImageJ, normalized to β-actin, and presented as mean ± SD relative expression levels from ≥ 3 independent experiments.

Seahorse extracellular flux analysis

The oxygen consumption rate (OCR) and extracellular acidification rate were assessed using a Seahorse XFe96 Analyzer. Cells were seeded at 10, 000 cells per well and incubated overnight. On the day of the assay, cells were washed and incubated in the Seahorse XF assay medium. Data were normalized to cell number.

Mitochondrial morphology

Samples were fixed in 2.5% glutaraldehyde, followed by post-fixing in osmium acid/potassium ferricyanide. They were then dehydrated using ethanol and acetone series. After infiltration with embedding medium and polymerization, ultrathin sections were cut and stained. A blinded observer then assessed mitochondrial morphology using a transmission electron microscope.

Mitochondrial damage and intracellular ROS assay

Cells were seeded at 1×10^6 cells/flask in T25 flasks. Mitochondrial membrane potential (MMP) was assessed using the JC-1 dye, and analyzed using flow cytometry. The ratio of red to green fluorescence (Q2%/Q3%) was calculated to determine changes in MMP. Intracellular ROS levels were measured using flow cytometry with the ROS-sensitive dye DCFDA. ROS-positive cells (M1%) and MFI were determined. MitoTracker™ is a red fluorescent dye that stains the mitochondria of living cells. Post-modeling, 1 mM MitoTracker was diluted in pre-warmed medium to 500 nM for staining.

Statistical analysis

Data are presented as mean ± standard deviation. Statistical analyses were performed using GraphPad Prism 9.0. Group comparisons were conducted using unpaired two-tailed t-tests or Mann-Whitney U tests. For multiple group comparisons, one-way ANOVA followed by Tukey's post hoc test was used. Correlations between variables were assessed using Pearson or Spearman correlation. A p-value of less than 0.05 was considered statistically significant.

Results

IR and Pyroptosis-Mediated inflammation in placentas

The clinical characteristics are summarized in Table 1. The GDM group exhibited significantly higher glucose levels on an oral glucose tolerance test (OGTT) at diagnosis, greater weight gain during pregnancy, higher levels of fasting plasma glucose, glycated hemoglobin (HbA1c), insulin, and homeostatic model assessment of insulin resistance (HOMA-IR), and a lower quantitative insulin sensitivity check index (QUICKI) at delivery compared to those of the NGT group.

Dual staining assays using TUNEL and caspase-1 (Fig. 1A-C), coupled with western blot evaluation of the GSDMD N-terminal fragment (Fig. 1D-E) indicated increased pyroptosis in GDM placentas compared to NGT placentas. ELISA revealed significantly higher levels of IL-1β and IL-18 in GDM placentas (Fig. 1F-G). There was a positive correlation between placental IL-1β and IL-18 levels (Fig. 1H). Both IL-1β and IL-18 correlated positively with the following: weight gain during pregnancy, OGTT (0 min glucose) at diagnosis, HbA1c, and logHOMA-IR at delivery; IL-1β and IL-18 correlated negatively with QUICKI at delivery (Fig. 2A-J). Additionally, IL-1β and IL-18 were positively correlated with other metabolic indicators, respectively (Fig. 2K). Although these correlations were weak, they could still point to trends meriting additional investigation. In the GDM group, placental IL-1β and IL-18 demonstrated a stronger correlation with fasting insulin and IR indexes at delivery, as compared to the overall dataset (Fig. 3A-F). Additionally, they were positively correlated with BMI and HbA1c at delivery in the GDM group (Fig. 3G-J). Compared to the overall dataset, the inter-correlation between IL-1β and IL-18 levels in the placentas of GDM patients is enhanced (Fig. 3K). These findings suggest that IR during gestation is closely linked to pyroptosis-mediated inflammation in placentas, particularly in GDM cases.

NLRP3-Related pyroptosis and mitochondrial damage in IR-mediated trophoblastic injury

After 48 h, glucose uptake in the 1000 nM insulin group rebounded compared to the 100 nM group, indicating the presence of compensatory mechanisms, similar to the hyperinsulinemia observed in vivo in IR (Fig. 4A). Furthermore, 1000 nM insulin treatment for 48 h caused a marked decrease in cell viability (Fig. 4B), reflecting cellular stress and toxicity induced by prolonged high

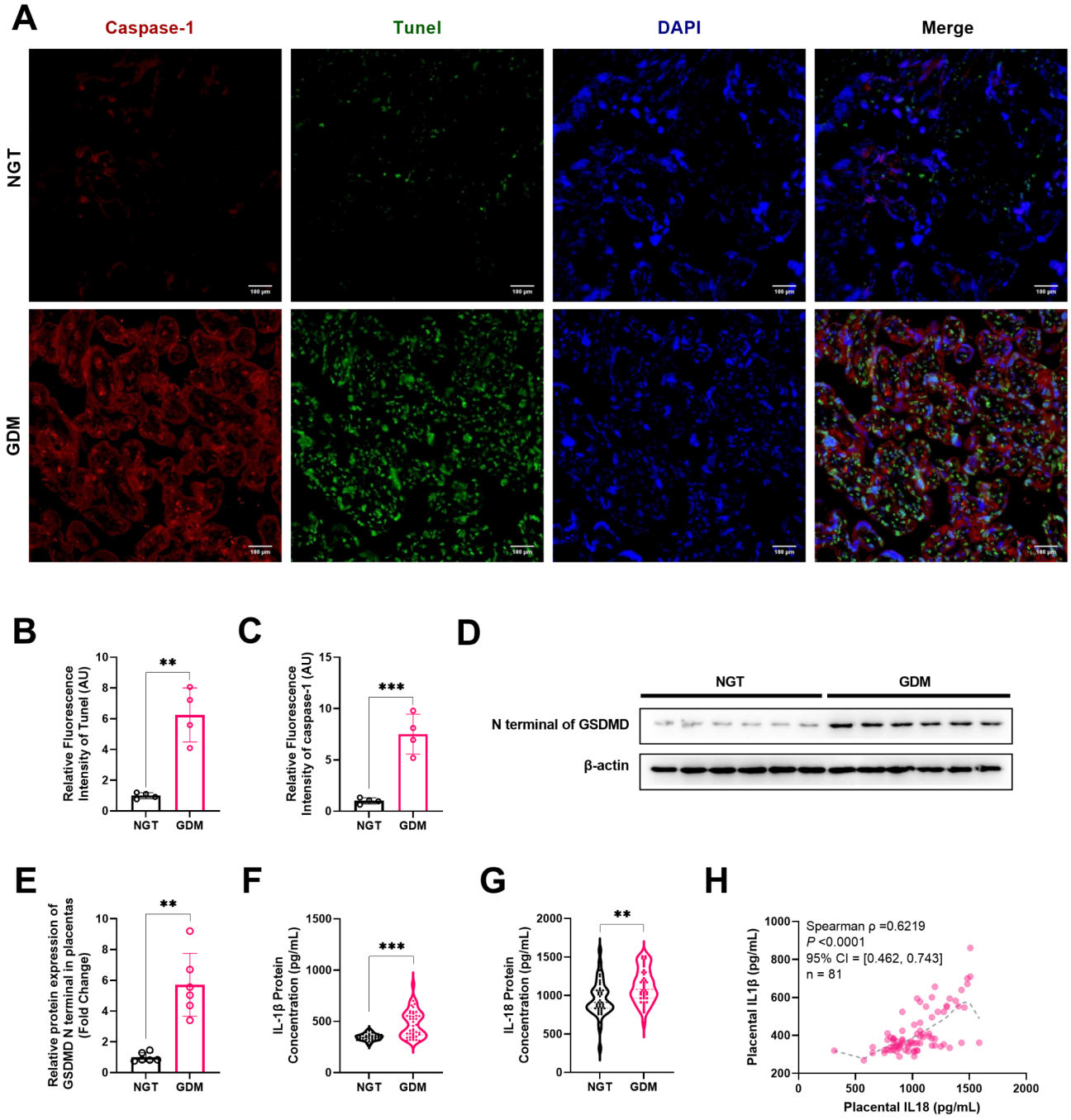

Fig. 1 Increased Pyroptosis in Placentas of GDM Patients. (**A**) Representative images and (**B**–**C**) quantification of fluorescence intensity of double-fluorescent staining for caspase-1 (red) and TUNEL (green) in the placentae from NGT and GDM patients. Scale bars: 100 μm. $n = 4$. (**D**–**E**) Western blot analysis showing increased N-terminal fragment of GSDMD protein expression levels in GDM placentas compared to that of NGT placentas. Data are presented as mean ± SD, $n = 6$. (**F**–**G**) ELISA analysis showing significantly higher expression levels of the pyroptosis-related inflammatory factors IL-1β and IL-18 in the placentas of GDM ($n = 42$) patients compared to those in the NGT ($n = 39$) group. (**H**) Spearman correlation analysis was performed to determine the relationship between IL-1β and IL-18 levels in placental tissue ($n = 81$). $^{**}P < 0.01$, $^{***}P < 0.001$ using unpaired two-sided t-test or Mann-Whitney test

insulin exposure, a key feature of IR. Therefore, subsequent experiments used 1000 nM insulin treatment for 48 h.

Western blot analysis confirmed the activation of the pyroptosis, with increased levels of NLRP3, cleaved caspase-1, and the N terminal fragment of GSDMD in insulin-treated trophoblasts (Fig. 4C-D). ELISA revealed elevated levels of IL-1β and IL-18 (Fig. 4E). Knocking down GSDMD in HTR-8 cells reduced LDH release and improved cell viability, highlighting pyroptosis

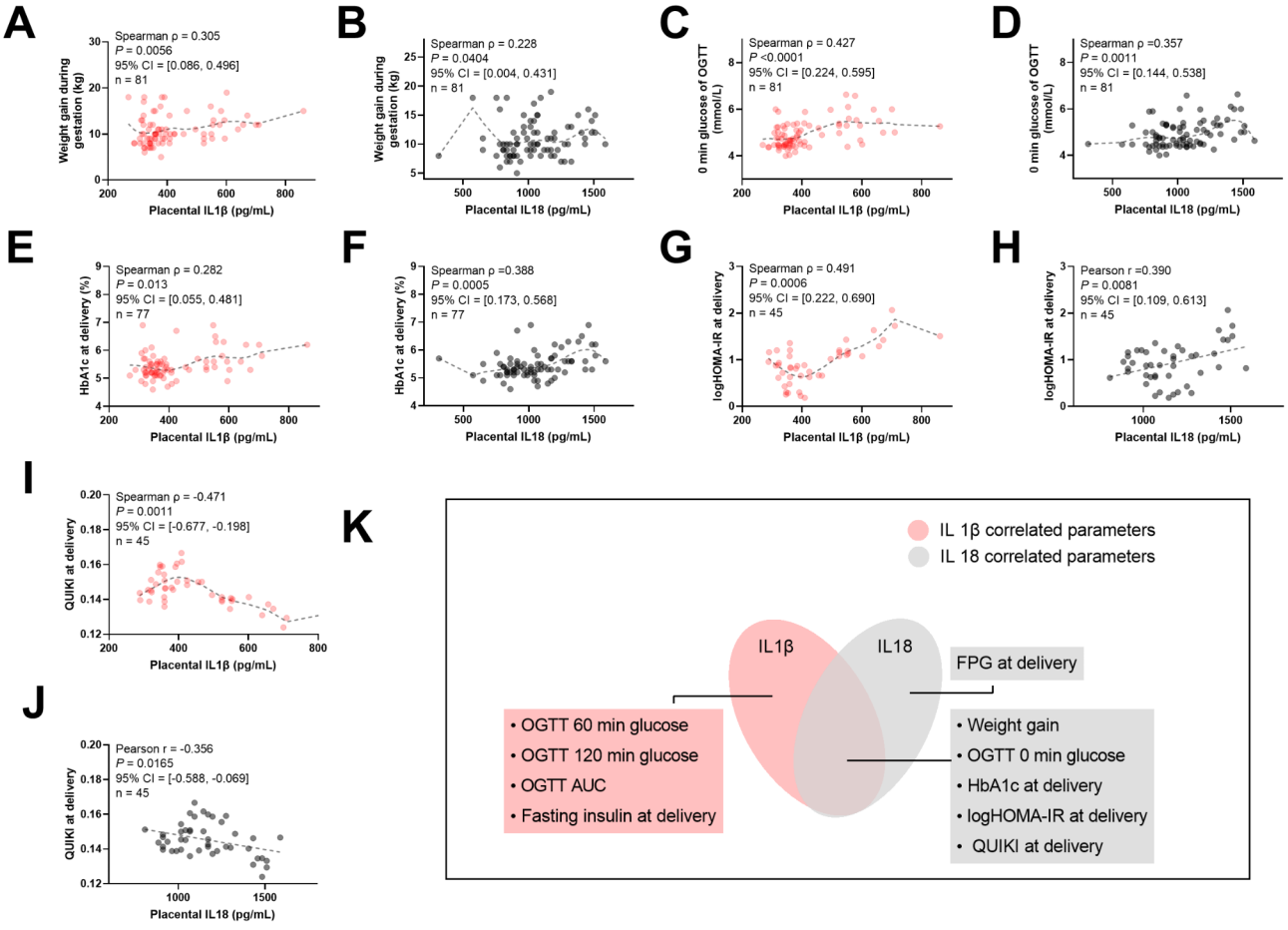

Fig. 2 Correlation of Placental Pyroptosis Markers with Clinical Indicators. (**A**–**J**) Positive correlations between placental IL-1β and IL-18 levels with weight gain during pregnancy, OGTT (0 min glucose) at diagnosis, HbA1c, and logHOMA-IR at delivery. Negative correlations between IL-1β and IL-18 levels with QUICKI at delivery were observed. (**K**) Venn diagram showing the clinical indicators correlated with IL-1β and IL-18

as one of the mechanism in IR-mediated trophoblast injury (Fig. 4F–G). The OCR serves as a direct measure of mitochondrial respiration and energy output, while the extracellular acidification rate is primarily related to lactate production, serving as an indicator of glycolytic activity. Seahorse XF analysis showed that IR decreased various OCR metrics, including basal respiration, ATP-linked respiration, and maximal respiration in trophoblasts, while glycolytic capacity remained unchanged (Fig. 4H-L).

Metformin mitigates IR-Induced pyroptosis and cellular damage in trophoblasts

We leveraged pharmacokinetic data from metformin studies in the placenta to establish a pharmacological concentration gradient (10, 50, and 100 μM), while also including a supra-therapeutic dose (1000 μM). HTR-8 cells were pre-treated with 1000 nM insulin for 48 h and metformin for an additional 24 h. Western blot analyses demonstrated that metformin — across a range of concentrations — suppressed IR-induced increases in NLRP3, cleaved caspase-1, and GSDMD-NT (Fig. 5A-D). The attenuation of IR-induced pyroptosis exhibited a U-shaped dose-response curve, with the optimal effect observed at 100 μM, and substantial efficacy also evident at the supra-therapeutic dose of 1000 μM. ELISA confirmed similar trends in IL-1β and IL-18 suppression (Fig. 5E-F).

Unlike the continuous attenuation of pyroptosis, metformin only began to mitigate insulin-induced declines in cell viability at certain concentrations (50–100 μM). Additionally, when metformin levels exceeded therapeutic thresholds, cell viability significantly decreased (Fig. 5G-H). For further experiments, we selected a metformin concentration of 100 μM. GSDMD suppression reduced LDH release and improved cell viability under IR-induced stress in the absence of metformin, with no significant difference between the IR + sh-GSDMD + Metformin and IR + sh-GSDMD groups (Fig. 5I-J). This observation aligns with Fig. 4F-G, confirming GSDMD suppression's protective effect on cell viability under IR stress. These findings indicated that metformin mitigates

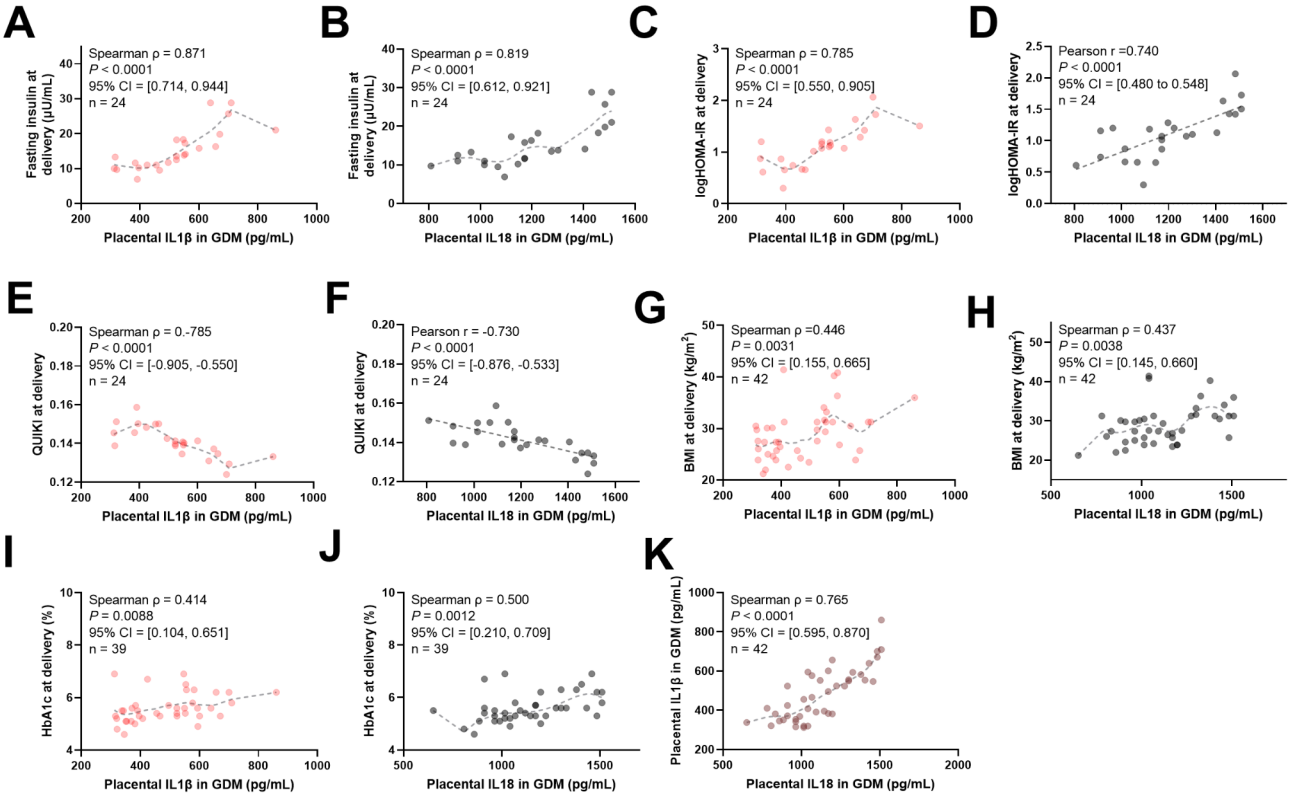

Fig. 3 Stronger Correlation of Pyroptosis Markers with IR in GDM Patients. (**A**–**F**) In the GDM group, placental levels of IL-1β and IL-18 show stronger correlations with fasting insulin and IR indices (logHOMA-IR and QUICKI) at delivery compared to that observed in all 81 samples. (G–J) Positive correlations of IL-1β and IL-18 levels with BMI and HbA1c at delivery. (**K**) Enhanced inter-correlation between IL-1β and IL-18 levels in the placentas of GDM patients compared to the overall dataset

IR-induced pyroptosis and cellular damage primarily through the NLRP3 pathway.

Metformin enhances mitochondrial biogenesis to alleviate IR-Induced mitochondrial damage in trophoblasts

Therapeutic metformin (10–100 μM) following insulin treatment increased basal, ATP-linked, and maximal OCR in trophoblasts compared to insulin alone. However, 1000 μM metformin, while enhancing basal and ATP-linked respiration, failed to restore maximal OCR impaired by IR (Fig. 6A-D). Glycolysis levels showed no significant changes across groups (Supplementary Fig. 1).

Electron microscopy revealed notable mitochondrial alterations in IR-treated trophoblasts, including swelling, irregular shapes, and reduced cristae (Fig. 6E). After treatment with metformin, although some damaged mitochondria were still present, the number of healthy mitochondria and total mitochondria appeared to increase. JC-1 flow cytometry showed that metformin partially restored MMP, although the effect was less pronounced at supra-therapeutic concentrations (Fig. 6F-G). Healthy mitochondria always have a high membrane potential, as indicated by a majority of the cells in the Q2 quadrant. Increased mitochondrial biogenesis is typically accompanied by more healthy mitochondria. Additionally, MitoTracker staining showed IR significantly decreased mitochondrial fluorescence, reflecting reduced mitochondrial quantity under IR stress. In contrast, treatment with 50 μM and 100 μM metformin increased mitochondrial fluorescence, suggesting enhanced mitochondrial biogenesis (Fig. 6H-I). Although a trend towards increased mitochondrial biogenesis was observed with 10 μM and 1000 μM metformin, the differences when compared to the IR group were not statistically significant. These results suggested that therapeutic metformin mitigates mitochondrial damage by promoting mitochondrial biogenesis.

Metformin protects against IR-Induced oxidative stress and TXNIP overexpression in trophoblasts

To evaluate oxidative stress, we measured intracellular ROS levels using flow cytometry, assessing both the percentage of ROS-positive cells (M1%) and the mean fluorescence intensity (MFI). IR significantly increased intracellular ROS levels, both in terms of M1% and MFI. Metformin (10–100 μM) reduced ROS levels, with the optimal effect occurring at 100 μM. At 1000 μM,

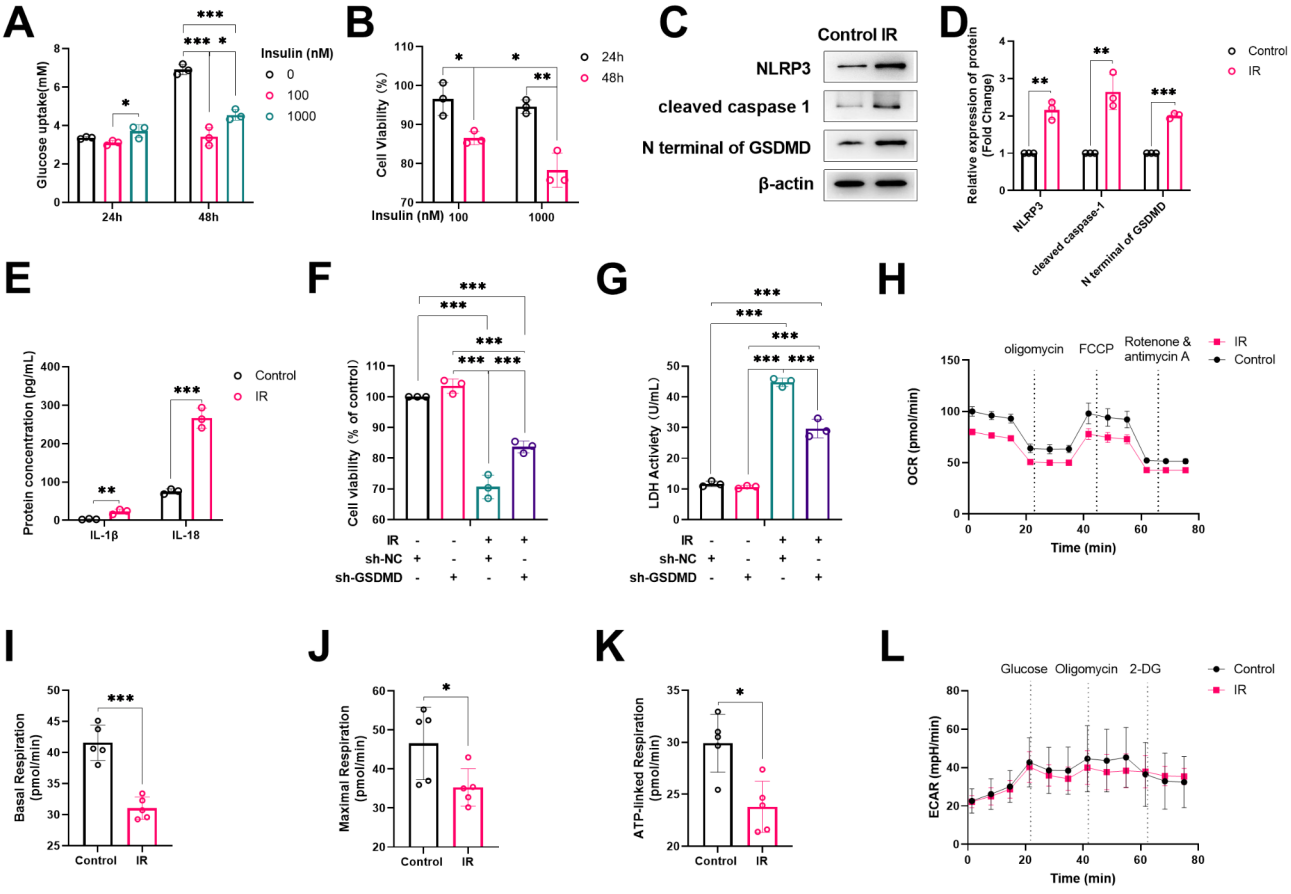

Fig. 4 NLRP3-Related Pyroptosis and Mitochondrial Damage in Trophoblasts under IR. (**A**) Glucose uptake assay. HTR-8/SVneo cells treated with insulin (100 nM and 1000 nM) for 24 and 48 h. ($n=3$). (**B**) Cell viability was measured with the Cell Counting Kit-8 (CCK-8) assay ($n=3$). (**C**–**D**) Western blot analysis showing increased activity of NLRP3, cleaved caspase-1, and N-terminal fragment of GSDMD in insulin-treated trophoblasts ($n=3$). (**E**) ELISA quantification of IL-1β and IL-18 in conditioned media from insulin-treated HTR-8/SVneo cells. ($n=3$). (**F**–**G**) GSDMD knockdown in HTR-8 cells mitigated IR-induced LDH release and cell viability loss induced by IR. ($n=3$). (**H**-**K**) The OCR assay was used to observe the mitochondrial respiratory function. The results showed significant decreases in basal respiration, ATP-linked respiration, and maximal respiration in the IR group compared to that of the control group. ($n=5$). (**L**) There was no significant alteration in the glycolytic capacity of HTR-8 cells in the IR group, as measured by extracellular acidification rate (ECAR) ($n=5$). Data are presented as mean ± SD. $^{*}P<0.05$, $^{**}P<0.01$, and $^{***}P<0.001$, using unpaired two-sided t-test for two-group comparisons, and one-way ANOVA coupled with Tukey's post hoc test for multiple group comparisons

metformin reduced M1% but had little effect on MFI (Fig. 7A-C).

TXNIP is a crucial regulator in oxidative stress pathways, with ROS promoting its upregulation. TXNIP expression, elevated by chronic high insulin exposure, was reduced by metformin at various concentrations, including at 1000 μM (Fig. 7D-E). Western blotting revealed increased TXNIP expression in GDM placentas compared to NGT placentas (Fig. 7F-G). These findings suggested that metformin exerts protective effects in insulin-treated trophoblasts by inhibiting the ROS/TXNIP pathway.

Metformin alleviates IR-Induced pyroptosis in trophoblasts via TXNIP

Dual immunofluorescence showed increased expression of TXNIP and NLRP3, along with an enhanced co-localization in IR-treated trophoblasts, which was reduced by metformin (100 μM) (Fig. 8A-C). To confirm that the protective effects of metformin against insulin-induced injury are TXNIP-dependent, we silenced TXNIP in HTR8 cells using siRNA. In the TXNIP-silenced groups, metformin treatment did not further mitigate insulin-induced NLRP3 elevation (Fig. 8A-C). Western blotting and Elisa assay further validated changes in pyroptosis-related proteins and inflammatory factors, showing that TXNIP knockdown had similar effects to metformin. Post-TXNIP knockdown, additional metformin treatment did not provide further alleviation (Fig. 8D-I). Similarly, LDH release and CCK8 assay results indicated no significant difference between the IR + Metformin + si-NC, IR + si-TXNIP, and IR + Metformin + si-TXNIP groups (Fig. 8J-K). In conclusion, our findings confirmed that metformin protects against

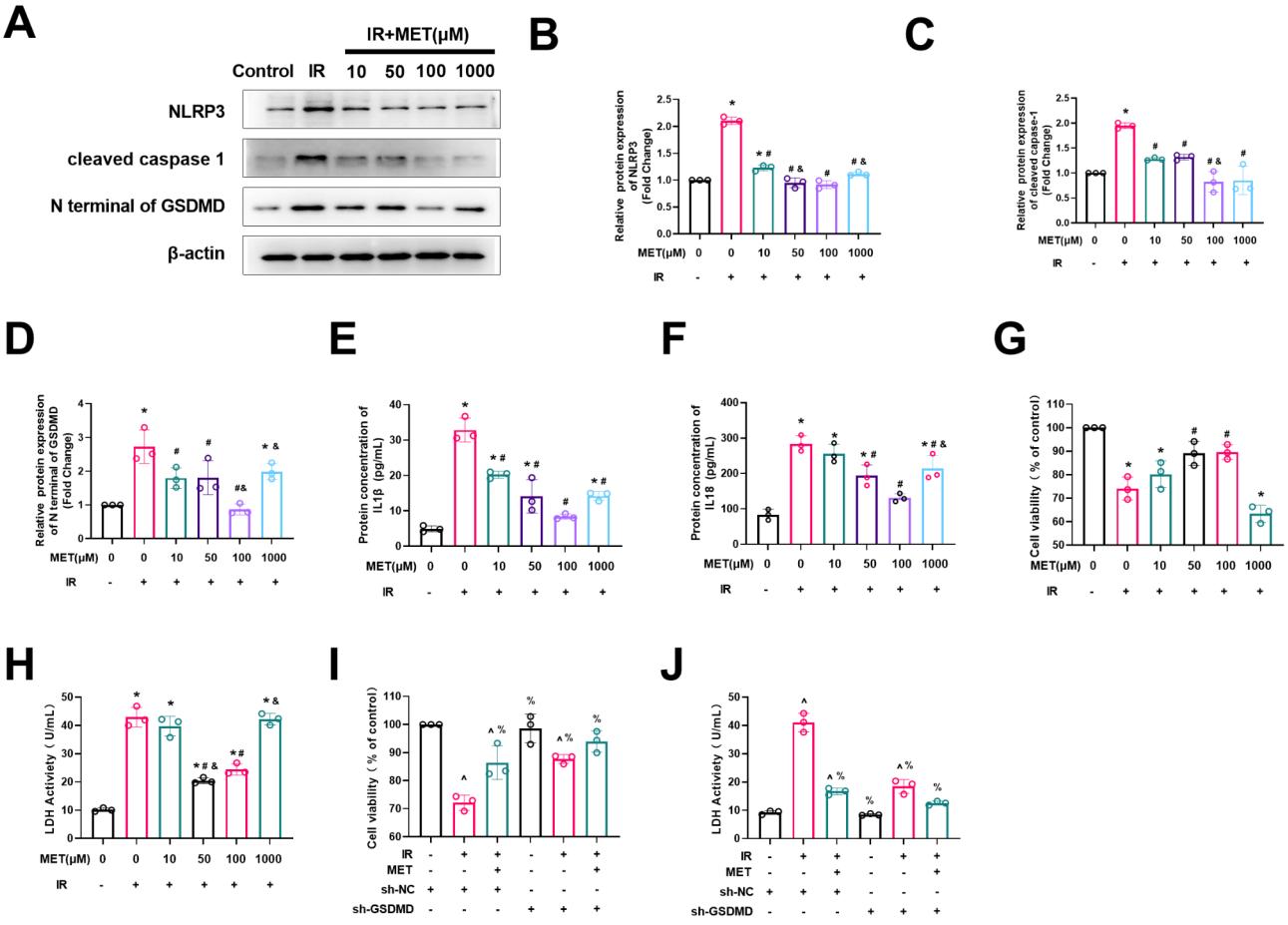

Fig. 5 Metformin Mitigates IR-Induced Pyroptosis and Cellular Damage in Trophoblasts. (**A**–**D**) Western blot analysis of pyroptosis-related protein, including NLRP3, cleaved caspase-1, and the N-terminal fragment of GSDMD, in HTR-8 cells treated with insulin (1000 nM) and varying concentrations of metformin (10, 50, 100, and 1000 μM). (**E**–**F**) ELISA measurements of pyroptosis-related inflammatory factors, IL-1β and IL-18, in conditioned media of HTR-8 cells. (**G**–**H**) Assessment of cell viability using CCK8 assays and LDH release measurements. (**I**–**J**) Cell viability assessment by CCK8 assays and LDH levels in HTR-8 cells with sh-GSDMD treatment to evaluate the role of NLRP3-induced pyroptosis in IR-induced trophoblast injury and its modulation by metformin (100 μM). Data are presented as mean ± SD, $n = 3$. $^{*}P < 0.05$ compared with no-treatment group; $^{\#}P < 0.05$ compared with IR group; $^{\&}P < 0.05$ compared with lower-dose group, lower-dose group refers to the concentration of metformin immediately lower in the gradient (e.g., 10 μM compared to 50 μM); $^{\wedge}P < 0.05$ compared with sh-NC group; $^{\%}P < 0.05$ compared with sh-NC + IR group. Statistical significance was determined using one-way ANOVA with Tukey's post hoc test

IR-induced pyroptosis by downregulating the TXNIP/NLRP3 pathway.

Discussion

This study investigated the effects of IR on mitochondrial function and pyroptosis in trophoblasts, along with the protective role of metformin. Our findings demonstrate that IR significantly impairs mitochondrial function and increases pyroptosis in trophoblasts. Metformin, particularly at therapeutic doses, mitigates mitochondrial dysfunction by promoting mitochondrial biogenesis and alleviates pyroptosis through the ROS/TXNIP/NLRP3 pathway in the context of IR (Fig. 8L). These results offer novel insights into the pathophysiology of GDM and support the therapeutic use of metformin in managing IR-related complication during pregnancy.

We observed a notable increase in pyroptosis in GDM placentas compared to those with NGT, with elevated IL-1β and IL-18 levels. In the GDM group, IL-1β and IL-18 levels were correlated more strongly with IR indices than with blood glucose control. This suggested that IR, independent of hyperglycemia, plays a crucial role in placental inflammation, and could explain the clinical observations of poor pregnancy outcomes in individuals with conditions like obesity and polycystic ovary syndrome, which are characterized by IR [22, 23].

Hyperinsulinemia exerts direct toxic effects on trophoblasts [24], which are linked to conditions like preeclampsia and miscarriage [25, 26]. Our study further demonstrated that insulin at IR levels activates the NLRP3 inflammasome, leading to pyroptosis in trophoblasts. This process was accompanied by significant

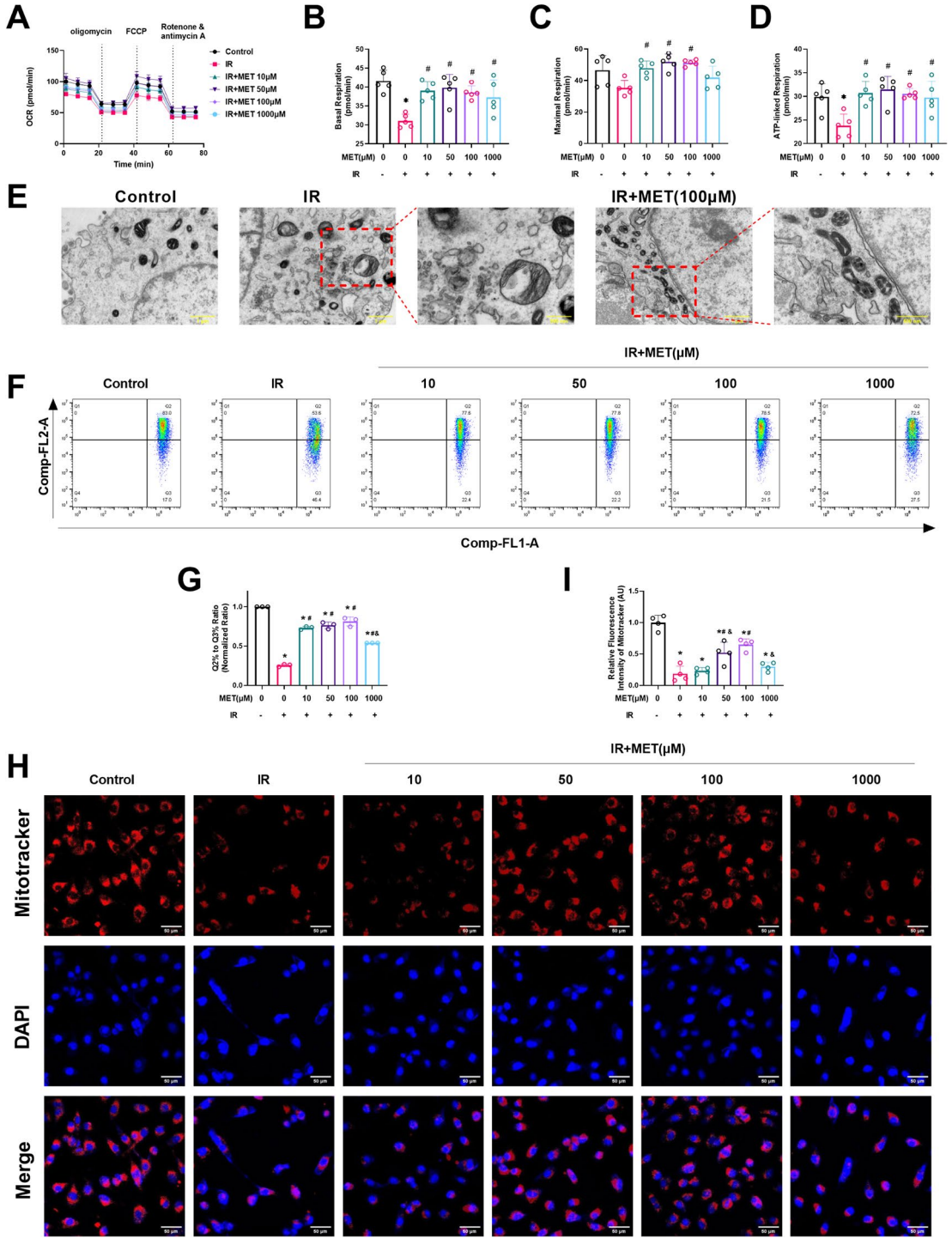

Fig. 6 Metformin Alleviate IR-Induced Mitochondrial Damage in Trophoblasts. (**A**–**D**) Oxygen Consumption Rate (OCR). Therapeutic concentrations of metformin (10–100 μM) significantly increased basal, ATP-linked, and maximal OCR compared to insulin alone. A concentration of 1000 μM metformin increased basal and ATP-linked respiration but failed to restore maximal OCR impaired by IR ($n=5$). (**E**) Electron microscopy images of trophoblast mitochondria. (**F**) Representative JC-1 flow cytometry analysis of MMP. (**G**) Ratio of cells in Q2 to Q3. Metformin partially restored MMP, indicated by a shift in the population of cells in the Q2 quadrant, but the effect was less pronounced at 1000 μM compared to that at lower concentrations ($n=3$). (**H**) Representative images and (**I**) quantification of fluorescence intensity of Mitotracker in trophoblasts. Scale bars: 50 μm. $n=4$. Data are presented as mean ± SD. $^{*}P<0.05$ compared with no-treatment group; $^{\#}P<0.05$ compared with IR group; $^{\&}P<0.05$ compared with lower-dose group, lower-dose group refers to the concentration of metformin immediately lower in the gradient (e.g., 10 μM compared to 50 μM); Statistical significance was determined using one-way ANOVA with Tukey's post hoc test

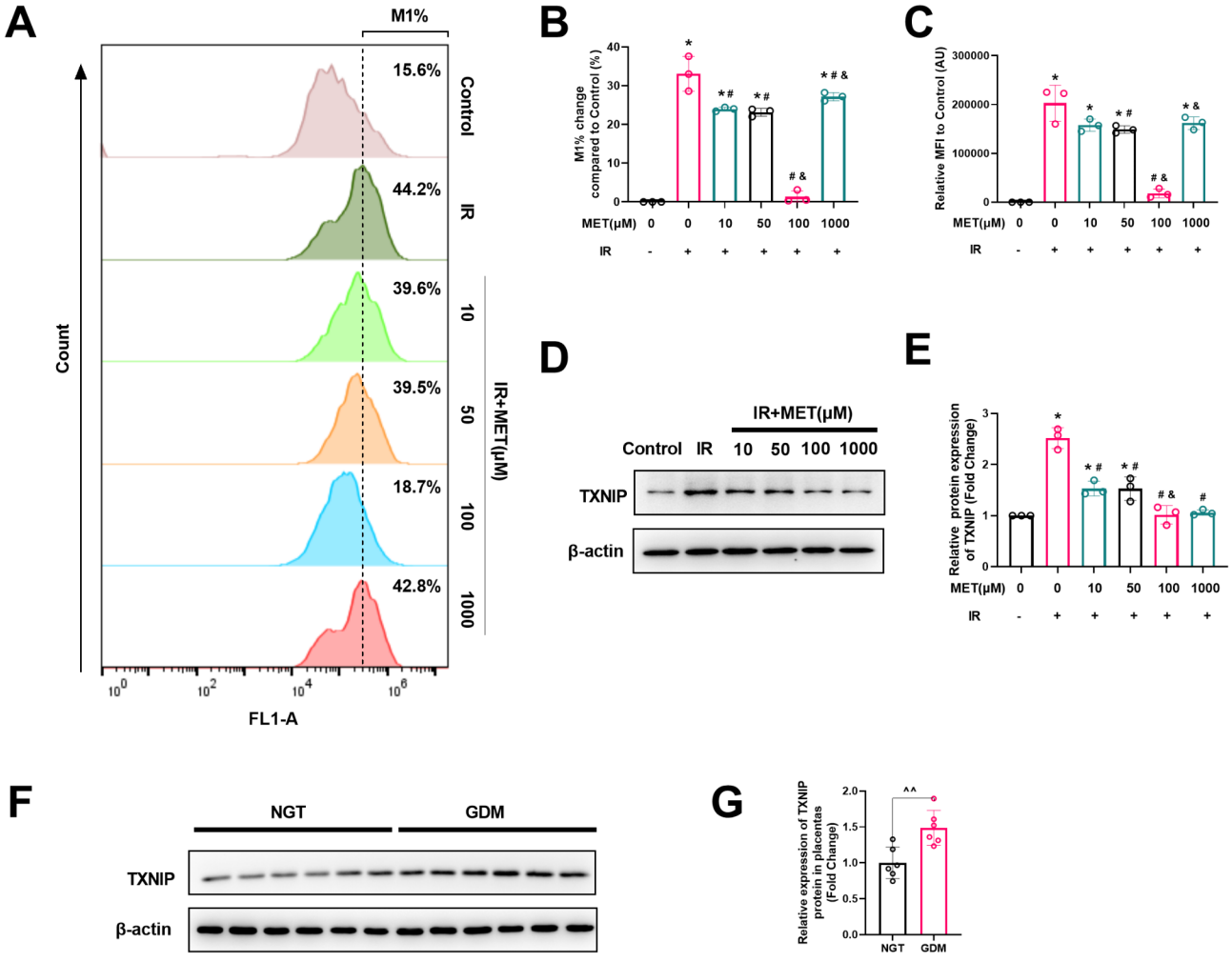

Fig. 7 Metformin Attenuates IR-Induced Oxidative Stress and TXNIP Overexpression in Trophoblasts. (**A**) Representative flow cytometry histograms displaying ROS levels in trophoblasts. (**A**) The percentage of ROS-positive cells (M1%) and (**C**) the mean fluorescence intensity (MFI). Insulin resistance (IR) significantly increased both M1% and MFI compared to controls. Metformin treatment at 10–100 μM significantly reduced both M1% and MFI, with optimal effects at 100 μM. At 1000 μM, metformin reduced M1%, but did not significantly impact MFI. (**D**-**E**) Western blots showing increased TXNIP levels in response to high insulin exposure, with metformin treatment at various concentrations (10–1000 μM) reducing TXNIP expression. Data of experiments in vitro are presented as mean ± SD, $n = 3$. $^{*}P < 0.05$ compared with no-treatment group; $^{\#}P < 0.05$ compared with IR group; $^{\&}P < 0.05$ compared with lower-dose group, lower-dose group refers to the concentration of metformin immediately lower in the gradient (e.g., 10 μM compared to 50 μM). Statistical significance was determined using one-way ANOVA with Tukey's post hoc test for multiple group comparisons. (**F**) Representative Western blots and (**G**) quantification of TXNIP protein expression showed elevated TXNIP protein levels in GDM placentas compared to that of NGT placentas. Data are presented as mean ± SD, $n = 6$. $^{\wedge\wedge}P < 0.01$ using unpaired two-sided t-test compared to NGT

mitochondrial dysfunction, evidenced by reduced basal respiration, ATP-linked respiration, and maximal respiration. Mitochondria play a central role in regulating cell death, differentiation, proliferation, and immune responses, and mitochondrial damage has been associated with GSDMD-mediated pyroptosis [15]. Thus, targeting mitochondrial function could be a promising strategy for addressing IR-related trophoblastic injury.

Metformin, a long-standing treatment for diabetes, is recognized for its role in inhibiting mitochondrial respiratory complex I, reducing ATP production, and activating the AMP-activated protein kinase pathway, which lowers oxidative stress and improves inflammatory responses [27]. However, metformin's effects on mitochondria are biphasic: at low concentrations (below 250 μM), it promotes mitochondrial biogenesis and increases oxygen consumption, while at higher concentrations (above 5000 μM), it inhibits mitochondrial respiration and induces metabolic reprogramming [28]. These findings were observed in cardiomyocytes, while the effects of metformin vary across different tissues. The tissue concentrations of metformin after oral administration are estimated at 50–100 μM [29], with placental concentrations in GDM patients being potentially lower (10–100 μM) [16]. Primary trophoblast cultures exposed to metformin at 10–100 μM show inhibited mitochondrial

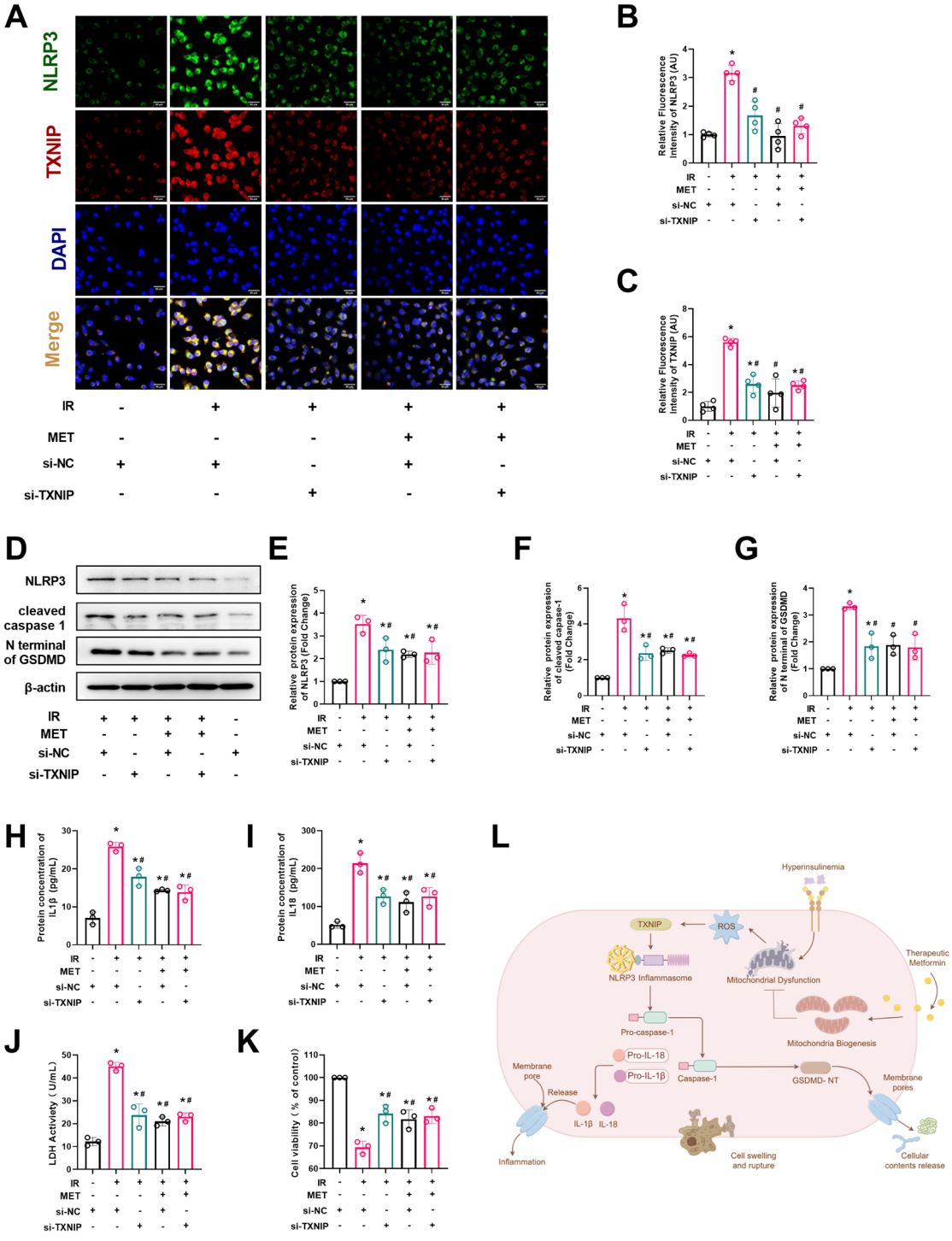

Fig. 8 Metformin Protects Trophoblasts from IR-Induced Pyroptosis via TXNIP inhibition. (**A**) Representative images of dual immunofluorescence of TXNIP (red) and NLRP3 (green) in trophoblasts. Metformin treatment (100 μM) significantly decreased the expression and interaction of these proteins. Scale bars: 50 μm. $n = 4$. (**B**-**C**) Quantification of TXNIP and NLRP3 expression levels. IR significantly increased the expression and interaction of TXNIP and NLRP3. In TXNIP-silenced groups, metformin treatment did not further mitigate insulin-induced NLRP3 elevation. (**D**–**G**). Western blotting of pyroptosis-related proteins. The protective effects of metformin against insulin-induced pyroptosis are TXNIP-dependent. (**H**–**I**) ELISA assay results for inflammatory factors IL-1β and IL-18 in conditioned media of cells. In TXNIP-silenced groups, metformin treatment did not further mitigate IL-1β and IL-18 elevation. Cell viability valued by (**J**) LDH release and (**K**) CCK8 assay. Metformin protects against IR-induced cell injury through TXNIP. Data are presented as mean ± SD, $n = 3$. $^{*}P < 0.05$ compared with si-NC group; $^{\#}P < 0.05$ compared with the si-NC + IR group using one-way ANOVA with Tukey's post hoc test. (**L**) Schematic diagram for protective properties of therapeutic metformin in mitigating IR-driven pyroptosis in trophoblasts, performed using Figdraw 2.0

respiratory function and reduced oxidative stress [16]. Other studies, however, suggest that the deleterious effects of metformin on mitochondrial respiration occur only at supra-therapeutic concentrations (above 100 μM or 2000 μM) [17, 18]. The impact of metformin on mitochondrial function and oxidative stress also appears to depend on maternal conditions: it shows protective effects in obesity, GDM, gestational hypertension, and hyperglycemia, but potentially harmful effects in healthy lean women [15, 18]. Our study confirmed that metformin improves IR-induced mitochondrial respiration and oxidative stress in trophoblasts, with therapeutic effects observed at concentrations between 10 and 100 μM, and even at supra-therapeutic concentrations (1000 μM). We also noted that chronic high insulin exposure disrupted mitochondrial morphology, while metformin at therapeutic doses enhanced mitochondrial biogenesis. These results suggested a complex interplay between metformin dosage, external conditions, and its effects on mitochondrial function.

In conditions such as diabetes, preeclampsia, and neurodegenerative diseases, mitochondrial dysfunction leads to increased ROS, which triggers the TXNIP-NLRP3 pathway, a key factor in chronic inflammation [30, 31]. Our findings indicated that the ROS/TXNIP/NLRP3 axis is engaged in trophoblasts under IR conditions, and that metformin reduces TXNIP expression and its interaction with NLRP3, thereby decreasing pyroptosis. In TXNIP-silenced groups, metformin did not further reduce NLRP3 activation, confirming that its protective effects depend on TXNIP. Targeting this pathway could offer new therapeutic approaches for reducing placental inflammation and improving pregnancy outcomes in GDM.

Our research highlights the potential of targeting the ROS/TXNIP/NLRP3 pathway to manage complications related to IR during pregnancy. While metformin is commonly used, our results hint at broader benefits in reducing IR-induced placental damage. However, genetic, environmental, and healthcare differences across populations require caution in generalizing these results. A limitation of this study is the use of the HTR-8/SVneo cell line, which does not fully replicate primary trophoblasts; future studies using primary trophoblasts or organoids are needed. Additionally, incomplete clinical data limited the sample size for correlation analyses. Larger, more diverse cohorts and long-term follow-up studies are essential to validate these findings and explore the transgenerational effects of mitigating IR-induced placental inflammation.

Conclusions

In conclusion, our study demonstrated two important effects of metformin therapy: that it alleviates IR-induced mitochondrial dysfunction by promoting mitochondrial biogenesis, and that it reduces pyroptosis by downregulating the ROS/TXNIP/NLRP3 pathway. These mechanisms are important for understanding GDM pathophysiology, and they suggest potential therapeutic benefits of targeting this pathway. Further research is necessary to validate these findings and assess the long-term effects of metformin use during pregnancy, particularly considering the variability in metformin concentrations and maternal conditions.

Abbreviations

GDM	Gestational diabetes mellitus
IR	Insulin resistance
T2DM	Type 2 diabetes
BMI	Body mass index
NLRP3	NOD-,LRR- and pyrin domain-containing 3
ROS	Reactive oxygen species
GSDMD	Gasdermin D
OCR	Oxygen consumption rate
TXNIP	Thioredoxin interacting protein
ELISA	Enzyme linked immunosorbent assay
LDH	Lactate dehydrogenase
TUNEL	Terminal deoxynucleotidyl transferase mediated dUTP Nick-End labeling
MFI	Mean fluorescence intensity
OGTT	Oral glucose tolerance test
HbA1c	Glycated hemoglobin
HOMA-IR	Homeostatic model assessment of insulin resistance
QUIKI	Quantitative insulin sensitivity check index
NGT	Normal glucose tolerance
MMP	Mitochondrial membrane potential

Supplementary Information

The online version contains supplementary material available at https://doi.org/10.1186/s12884-025-07419-0.

Supplementary Material 1: Figure 1: Glycolysis levels across all treatment groups ($n = 5$).

Supplementary Material 2

Supplementary Material 3

Acknowledgements

The authors acknowledge the assistance of Figdraw 2.0 (https://www.figdraw.com) in the creation of the mechanism diagrams presented in this paper.

Author contributions

RD, YB, and YS were responsible for data collection and experimental implementation. RD prepared the initial draft of the manuscript. LL and NW contributed to the discussion, oversaw the research, and offered essential revisions. All authors contributed significantly to the study's conceptualization and design, participated in either drafting or critically revising the manuscript for key intellectual content, and approved the final version for submission.

Funding

This study was funded by the National Natural Science Foundation of China (Grant Nos. 82200930, 82300933 and 81700706), as well as the Science Foundation of the Liaoning Department of Science and Technology (Grant Nos. 2023JH2/101700125, 2023JH2/101700119, and 2024JH2/102600326). Additional support was provided by the 345 Talent Project of Shengjing

Hospital and the Clinical Research Project of the Liaoning Diabetes Medical Nutrition Prevention Society (No.LNSTNBYXYYFZXH-RS02A and RS01B).

Data availability
The data supporting the findings of this study are available from the corresponding author upon reasonable request.

Declarations

Ethics approval and consent to participate
The project was in accordance with the Declaration of Helsinki and approved by the Ethics Committee of Shengjing Hospital of China Medical University (2016PS360K). Informed consent was obtained from all participants.

Consent for publication
Not applicable.

Competing interests
The authors declare no competing interests.

Received: 24 November 2024 / Accepted: 4 March 2025
Published online: 15 March 2025

References

1. Bianco ME, Kuang A, Josefson JL, Catalano PM, Dyer AR, Lowe LP, et al. Hyperglycemia and adverse pregnancy outcome Follow-Up study: newborn anthropometrics and childhood glucose metabolism. Diabetologia. 2021;64(3):561–70.
2. Wang H, Li N, Chivese T, Werfalli M, Sun H, Yuen L, et al. IDF diabetes atlas: Estimation of global and regional gestational diabetes mellitus prevalence for 2021 by international association of diabetes in pregnancy study group's criteria. Diabetes Res Clin Pract. 2022;183:109050.
3. American Diabetes Association Professional Practice C. 15. Management of diabetes in pregnancy: standards of care in diabetes-2024. Diabetes Care. 2024;47(Suppl 1):S282–94.
4. Johns EC, Denison FC, Norman JE, Reynolds RM. Gestational diabetes mellitus: mechanisms, treatment, and complications. Trends Endocrinol Metabolism. 2018;29(11):743–54.
5. Choudhury AA, Rajeswari VD. Polycystic ovary syndrome (PCOS) increases the risk of subsequent gestational diabetes mellitus (GDM): A novel therapeutic perspective. Life Sci. 2022;310:121069.
6. Du R, Li L. Estimating the risk of insulin requirement in women complicated by gestational diabetes mellitus: A clinical nomogram. Diabetes Metab Syndr Obes. 2021;14:2473–82.
7. Jiang L, Li AQ. Characteristics and pregnancy outcomes of subtypes of gestational diabetes mellitus based on HOMA-IR and BMI. Arch Gynecol Obstet. 2024;310(5):2355–61.
8. Lee K, Kuang A, Bain JR, Hayes MG, Muehlbauer MJ, Ilkayeva OR, et al. Metabolomic and genetic architecture of gestational diabetes subtypes. Diabetologia. 2024;67(5):895–907.
9. Wang JJ, Wang X, Li Q, Huang H, Zheng QL, Yao Q, et al. Feto-placental endothelial dysfunction in gestational diabetes mellitus under dietary or insulin therapy. BMC Endocr Disord. 2023;23(1):48.
10. Bucher M, Montaniel KRC, Myatt L, Weintraub S, Tavori H, Maloyan A. Dyslipidemia, insulin resistance, and impairment of placental metabolism in the offspring of obese mothers. J Dev Origins Health Disease. 2020;12(5):738–47.
11. Lu L, Zhang Y, Tan X, Merkher Y, Leonov S, Zhu L, et al. Emerging mechanisms of pyroptosis and its therapeutic strategy in cancer. Cell Death Discov. 2022;8(1):338.
12. Wu W, Tan QY, Xi FF, Ruan Y, Wang J, Luo Q, et al. NLRP3 inflammasome activation in gestational diabetes mellitus placentas is associated with hydrogen sulfide synthetase deficiency. Exp Ther Med. 2022;23(1):94.
13. Meng Q, Shao L, Luo X, Mu Y, Xu W, Gao C, et al. Ultrastructure of placenta of gravidas with gestational diabetes mellitus. Obstet Gynecol Int. 2015;2015:283124.
14. Muralimanoharan S, Maloyan A, Myatt L. Mitochondrial function and glucose metabolism in the placenta with gestational diabetes mellitus: role of miR-143. Clin Sci (Lond). 2016;130(11):931–41.
15. Zhang Y, Liu W, Zhong Y, Li Q, Wu M, Yang L, et al. Metformin corrects glucose metabolism reprogramming and NLRP3 Inflammasome-Induced pyroptosis via inhibiting the TLR4/NF-kappaB/PFKFB3 signaling in trophoblasts: implication for a potential therapy of preeclampsia. Oxid Med Cell Longev. 2021;2021:1806344.
16. Tarry-Adkins JL, Robinson IG, Reynolds RM, Aye ILMH, Charnock-Jones DS, Jenkins B, et al. Impact of Metformin treatment on human placental energy production and oxidative stress. Front Cell Dev Biology. 2022;10:935403.
17. Nashif SK, Mahr RM, Jena S, Jo S, Nelson AB, Sadowski D, et al. Metformin impairs trophoblast metabolism and differentiation in a dose-dependent manner. Front Cell Dev Biology. 2023;11:1167097.
18. Hebert JF, Myatt L. Metformin impacts human syncytiotrophoblast mitochondrial function from pregnancies complicated by obesity and gestational diabetes mellitus in a sexually dimorphic manner. Antioxid (Basel). 2023;12(3):719.
19. Du R, Wu N, Bai Y, Tang L, Li L. circMAP3K4 regulates insulin resistance in trophoblast cells during gestational diabetes mellitus by modulating the miR-6795-5p/PTPN1 axis. J Transl Med. 2022;20(1):180.
20. Bai Y, Du Q, Zhang L, Li L, Wang N, Wu B, et al. Silencing of ANGPTL8 alleviates insulin resistance in trophoblast cells. Front Endocrinol (Lausanne). 2021;12:635321.
21. Yudhani RD, Sari Y, Nugrahaningsih DAA, Sholikhah EN, Rochmanti M, Purba AKR, et al. In vitro insulin resistance model: A recent update. J Obes. 2023;2023:1964732.
22. Catalano PM, Shankar K. Obesity and pregnancy: mechanisms of short term and long term adverse consequences for mother and child. BMJ. 2017;356:j1.
23. Bahri Khomami M, Shorakae S, Hashemi S, Harrison CL, Piltonen TT, Romualdi D, et al. Systematic review and meta-analysis of pregnancy outcomes in women with polycystic ovary syndrome. Nat Commun. 2024;15(1):5591.
24. Vega M, Mauro M, Williams Z. Direct toxicity of insulin on the human placenta and protection by Metformin. Fertil Steril. 2019;111(3):489–96. e5.
25. Zhang Y, Zhao W, Xu H, Hu M, Guo X, Jia W, et al. Hyperandrogenism and insulin resistance-induced fetal loss: evidence for placental mitochondrial abnormalities and elevated reactive oxygen species production in pregnant rats that mimic the clinical features of polycystic ovary syndrome. J Physiol. 2019;597(15):3927–50.
26. Kayashima Y, Townley-Tilson WHD, Vora NL, Boggess K, Homeister JW, Maeda-Smithies N, et al. Insulin elevates ID2 expression in trophoblasts and aggravates preeclampsia in obese ASB4-Null mice. Int J Mol Sci. 2023;24(3):2149.
27. Foretz M, Guigas B, Viollet B. Metformin: update on mechanisms of action and repurposing potential. Nat Rev Endocrinol. 2023;19(8):460–76.
28. Emelyanova L, Bai X, Yan Y, Bosnjak ZJ, Kress D, Warner C, et al. Biphasic effect of Metformin on human cardiac energetics. Transl Res. 2021;229:5–23.
29. LaMoia TE, Shulman GI. Cellular and molecular mechanisms of Metformin action. Endocr Rev. 2021;42(1):77–96.
30. Yang C, He Y, Ren S, Ding Y, Liu X, Li X, et al. Hydrogen attenuates cognitive impairment in rat models of vascular dementia by inhibiting oxidative stress and NLRP3 inflammasome activation. Adv Healthc Mater. 2024;13(20):e2400400.
31. Cheng SB, Nakashima A, Huber WJ, et al. Pyroptosis is a critical inflammatory pathway in the placenta from early onset preeclampsia and in human trophoblasts exposed to hypoxia and Endoplasmic reticulum stressors. Cell Death Dis. 2019;10(12):927.

Publisher's note